Highly reproducible SERS substrate based on polarization-free Ag nanoparticles decorated SiO2/Si core-shell nanowires array

Xiao-Ying Liu, Jian-An Huang, Bo Yang, Xue-Jin Zhang, and Yong-Yuan Zhu

---

Articles you may be interested in

Highly reproducible SERS substrate based on polarization-free Ag nanoparticles decorated SiO₂/Si core-shell nanowires array

Xiao-Ying Liu,[1,a] Jian-An Huang,[1,2,a] Bo Yang,[1] Xue-Jin Zhang,[1,b] and Yong-Yuan Zhu[1,c]

[1]*Key Laboratory of Modern Acoustics and National Laboratory of Solid State Microstructures, School of Physics, Nanjing University, Nanjing 210093, China*
[2]*Department of Electrical and Electronic Engineering, University of Hong Kong, Hong Kong SAR, China*

SiO₂/Si core-shell nanowires array coated with gap-rich silver nanoparticles were demonstrated as a highly reproducible surface-enhanced Raman scattering (SERS) substrate. SERS detection of a relative standard deviation of 8% for 10^{-4} M R6G with a spot size of ~2 μm and 900 spots over an area of 150×150 μm^2 was reported. The high reproducibility is ascribed to the polarization-independent electrical field distribution among three-dimensional nanowire structure with an optimized thickness of SiO₂ shell layer. © 2015 Author(s). All article content, except where otherwise noted, is licensed under a Creative Commons Attribution 3.0 Unported License. [http://dx.doi.org/10.1063/1.4921943]

Surface enhanced Raman scattering (SERS) relies on hot spots to identify the chemical fingerprints.[1] The hot spots have extremely strong electric field and are usually generated by localized surface plasmon resonance (LSPR). The electrical field coupling of LSPR in the gap of metal nanoparticle dimmer can result in a field enhancement up to 10^8.[1,2] Although single-molecule SERS detection could be realized with strong coupled LSPR field, the signals were often accompanied with low reproducibility and poor stability.[3] The commonly used solid-state SERS substrates offer highly ordered metal nanostructures for the generation of relatively uniform hot spots, such as silver nanoparticles (AgNPs) array,[4–7] silver nanotriangles array,[8] and silver film-over-nanosphere (AgFON).[1] However, the SERS performance of the above gap-based structures is closely related to the polarization of incident laser. The highest electric field enhancement appears if the excitation polarization is parallel to the metal nanoparticle dimmer axis.[9] This leads to polarization-dependent SERS signals in spot-to-spot Raman detection, which results in low signal reproducibility.

In this letter, we developed hexagonal-packed SiO₂/Si core-shell nanowires array with AgNPs decoration (AgNPs@SiO₂/SiNWs array) as a high reproducible gap-based SERS substrate. Here the optical mode guided along the direction of nanowire axis participates in the enhancement process. As a result, strong coupled electrical field can be generated in the gaps between neighboring AgNPs aligned along the direction of nanowire axis. The enhanced field can also be induced in the gaps of adjacent AgNPs within the cross section of the nanowire which originates from the direct excitation of incident laser. These two factors will contribute to the SERS. By adjusting the SiO₂ thickness, a polarization insensitive gap-based SERS substrate with high reproducibility can be realized.

The silicon nanowires array was first fabricated by nanosphere lithography and metal-assisted chemical etching,[10] and then the substrate was annealed at 900°C and 1 Bar in air for 2 hours to form an oxide layer on silicon surface. After that, the SiO₂/SiNWs array was covered with silver

---

[a]X. Y. Liu and J. A. Huang contributed equally to this work.
[b]Email: xuejinzh@nju.edu.cn
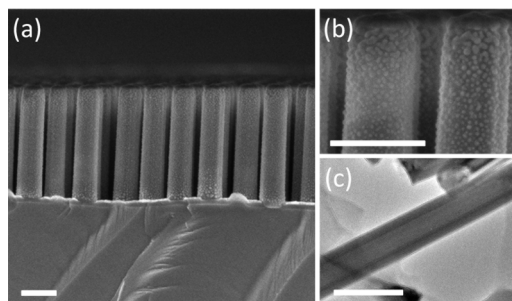[c]Email: yyzhu@nju.edu.cn

FIG. 1. (a) Cross-sectional SEM image of Ag nanopar ticle decorated SiO$_2$/SiNWs of 150 nm in diameter and ~1 μm^2 in length and (b) hexagonally packed AgNPs@SiO$_2$/SiNWs at 52° visual angle and (c) TEM image of SiO$_2$/Si nanowire after 2 hours annealing, the thickness of SiO$_2$ layer is ~40 nm. Scale bars are 200 nm.

by ion beam sputtering at an optimized duration of 4 min under 7 kev and 300 μA. As shown in Fig. 1(a), the as-fabricated AgNPs@SiO$_2$/SiNWs was hexagonally packed with an areal density of 12.8 wires/ μm^2. The wire diameter and length are respectively ~150 nm and ~1 μm. The scanning electron microscope (SEM) image (Fig. 1(b)) indicates that high density AgNPs were uniformly distributed on the surface of the hexagonal-packed SiO$_2$/SiNWs. The thickness of SiO$_2$ layer is ~40 nm after 2 hours' annealing, which is confirmed by transmission electron microscope (TEM) measurements as shown in Fig. 1(c).

The SERS measurements were performed with a confocal Raman system (Horiba Scientific, LabRAM HR Raman spectrometer). A 2 μL aqueous solution of Rhodamine 6G (R6G, Sigma-Aldrich) was dropped onto the substrate, spreading out as a circle of ~7 mm in diameter. After evaporation, the sample was excited by a He-Ne laser at wavelength of 633 nm via 50× and 10× objectives for Raman signal detection.

To evaluate the spot-to-spot SERS reproducibility of AgNPs@SiO$_2$/SiNWs array, we carried out mapping measurements of Raman signals with a spot size of ~2 μm over 150×150 μm^2 under a 50× objective and ~4 μm over 450×450 μm^2 under a 10× objective, respectively. Another ordered gap-based SERS substrate, AgFON, which was made by coating ~120-nm-thick silver layer on hexagonal-packed polystyrene nanospheres of 300 nm in diameter, was prepared for the control experiments. A comparison between them with regard to 1362 cm^{-1} peak of R6G (10^{-4} M) is shown in Fig. 2. Figure 2(a) exhibits high uniform R6G spectra from AgNPs@SiO$_2$/SiNWs array with RSD of 8.3% under a 50× objective. The RSD value changes a little with the laser spot. For example, the RSD was measured to be 8.7% when a 10× objective was used, as shown in Fig. 2(b). In contrast, the RSDs of R6G spectra from the AgFON (Fig. 2(c)) was measured as 32.1% under a 50× objective, whereas the RSD decreased to be 13.9% (Fig. 2(d)) under a 10× objective. The difference between Figs. 2(c) and 2(d) can be explained by the averaging effect.[11] The above results show that the AgNPs@SiO$_2$/SiNWs array structure is superior to the AgFON structure as for the performance of reproducibility, which can be maintained at a spot size as small as ~2 μm. To calculate the enhancement factor (EF), 4-Aminothiophonol (4-ABT) was used as the probe molecule for it can form a monolayer on the Ag surface.[4] The experimental Raman EF was calculated to be 6×10^5.[12]

We further studied the influence of the concentrations of R6G aqueous solution on the SERS spectra of on AgNPs@SiO$_2$/SiNW array. Figure 3(a) shows the SERS spectra for four different concentrations of R6G aqueous solution. The integration time is 5s. Figure 3(b) illustrates a mapping measurement with 10^{-6} M R6G aqueous solution, and the RSD is calculated as ~7%. Above results shows that the reproducibility can keep very high for the concentration of R6G aqueous solution as low as 10^{-6} M.

The core-shell structure of AgNPs@SiO$_2$/SiNWs SERS array was investigated by the simulation based on three-dimensional finite-difference time-domain (FDTD) software (Lumerical FDTD Solutions). The structures and geometrical parameters correspond to those in experiments, i.e., SiO$_2$/Si core-shell nanowires of 150 nm in outside diameter and 1 μm in length with different thicknesses of SiO$_2$ layer are close packed with AgNPs. The diameter and interval distance of AgNPs are
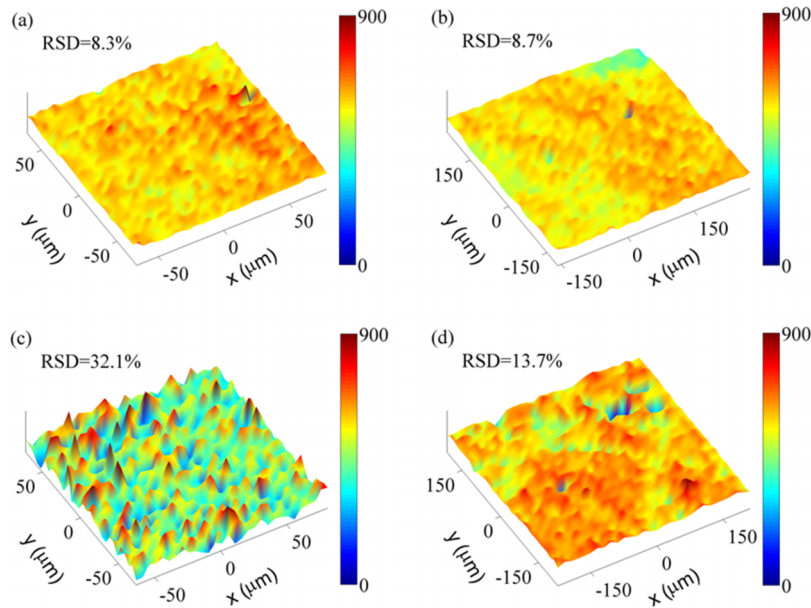
FIG. 2. Raman mapping images of 1362 cm^{-1} band of R6G from substrates of AgNPs@SiO2/SiNWs array under (a) a 50×
objective and (b) a 10× objective, and AgFON under (c) a 50× objective and (d) a 10× objective.

set as 20 nm and 13 nm respectively. The light source is an x-polarized plane wave at wavelength of
633 nm. Figure 4 shows the electrical field intensity distribution for three representative nanowires.
For silicon nanowire, the coupled LSPR electrical field in the gap of AgNPs is degenerated in
the cross section of an AgNPs@SiO$_2$/SiNW, as shown in Fig. 4(a). At wavelength of 633 nm, the
refractive index of Si is about 3.88, while that of SiO$_2$ is about 1.46. Thus the AgNPs@SiO$_2$/SiNWs
with thin SiO$_2$ shell layer, i.e. thick Si core, is likely to support guided modes.[13] The degeneration
of electrical field in the cross section (Fig. 4(a)) comes from the generation of guided mode along
the nanowire, which results in the redistribution of the electrical field. Being associated with the
guided mode, strong coupled electrical field can distribute in the gap of AgNPs dimmers aligned
along the nanowire axis direction, which is confirmed by Fig. 4(b). By comparison, for a SiO$_2$
nanowire, the coupled LSPR electrical field occurs in the gap of AgNPs, consistent with the incident
polarization, as shown in Fig. 4(c). Figure 4(d) presents weak electrical field distributed along the
nanowire axis direction in the absence of guided modes. It is expected that there is an intermediate
thickness of SiO$_2$ shell layer that the above two factors work together to generate a uniform field
enhancement around the nanowire surface. Figures 4(e) and 4(f) refer to an intermediate case of
core-shell SiO$_2$/SiNWs with 45 nm SiO$_2$ shell layer. It can be seen that both the electrical field
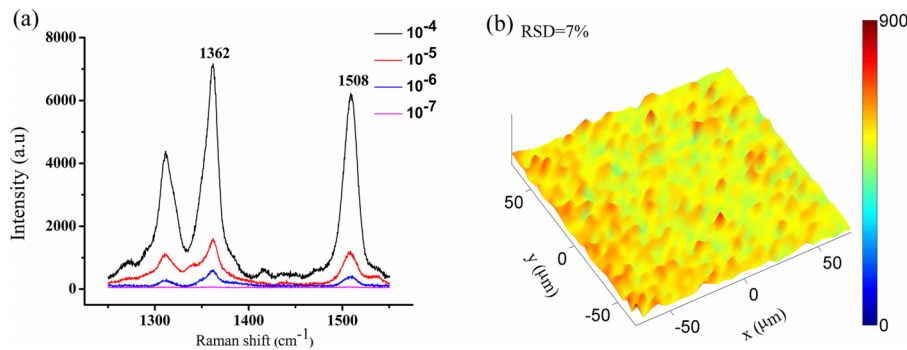

FIG. 3. (a) Spectra of evaporated R6G aqueous solution with different concentrations on AgNPs@SiO2/SiNWs array. (b)
Raman mapping image of 10^{-6}M R6G 1362 cm^{-1} band of R6G from AgNPs@SiO2/SiNWs array under 50× objective.
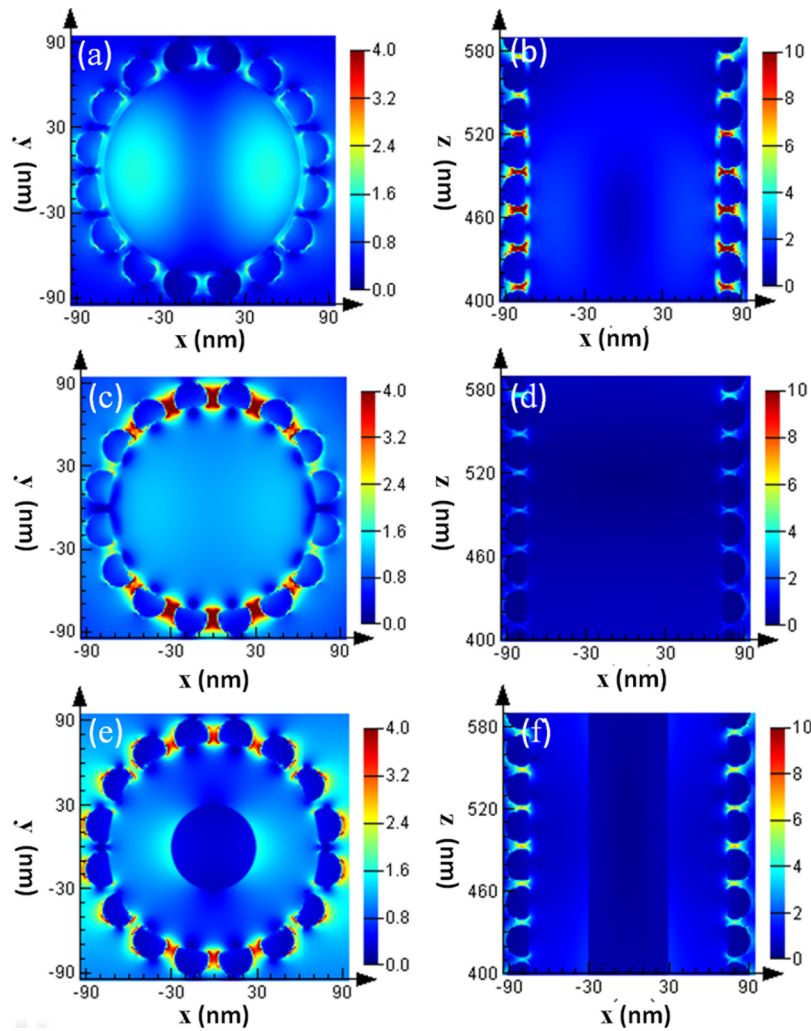
FIG. 4. Electrical field intensity distribution in the cross-sectional and vertical directions of (a, b) Si nanowire and (c, d) SiO$_2$ nanowire and (e, f) SiO$_2$/Si core-shell nanowire. The excitation light is x-polarized.

intensities in the cross-sectional and vertical directions are rather strong. The strong field enhances the Raman scattering. The Raman photons emitted from R6G inside the gap of AgNPs would be either absorbed or experience multiple scattering. Those escaped from the hexagonal-packed nanowire array would thus contribute to the detected Raman signal. Figures 4(e) and 4(f) also show that the electrical field is distributed with weakened anisotropy three-dimensionally. It will lead to the polarization independence and consequently the high SERS reproducibility.

The above analyses suggest an optimum thickness of SiO$_2$ shell layer that gives rise to uniformly distributed hot spots around the SiO$_2$/Si core-shell nanowire surface, hence the most reproducible SERS detection. This was experimentally verified by several SiO$_2$/SiNWs array substrates. The samples were treated by thermal annealing with annealing periods varied from 0 to 4 hrs at 900°C and 1 Bar in air, resulting in different thickness of SiO$_2$ shell layer. Other experimental processes are the same as the above-mentioned. SERS measurements were taken with a spot size of ~2 μm over 150×150 μm^2 under a 50× objective. Figure 5 shows that the highest reproducibility with the RSD value as low as 8% takes place for the annealing duration of 2-3 hrs. It also shows that the SERS-active capability of AgNPs@SiO$_2$/SiNWs array (Fig. 5(a)) is better than that of AgNPs/SiNWs array (Fig. 5(b)). The polarization-independent "hot spots" generation may account for the above behavior.
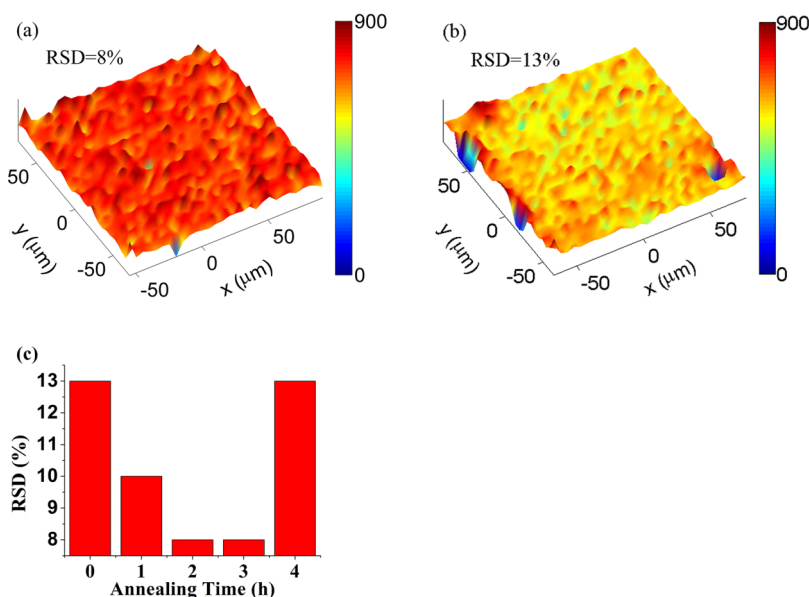
FIG. 5. Raman mapping images of 1362 cm^{-1} band of R6G from substrates of (a) AgNPs@SiO$_2$/SiNWs array (2 hrs annealing), and (b) AgNPs/SiNWs array (0 hrs annealing). (c) Relationship between the annealing period and the measured RSDs.

In conclusion, we characterized the RSD of SERS signals from AgNPs@SiO$_2$/SiNWs array substrates. With the optimization of SiO$_2$ shell layer, the RSD decreases to 8% from original 13% of AgNPs@SiNWs array substrates. This stems from the tunability of three-dimensional distribution of hot spots around the nanowire surface. The developed AgNPs@SiO$_2$/SiNWs array substrates may serve as practical SERS detection with high reproducibility.

ACKNOWLEDGEMENT

[1] S. L. Kleinman, R. R. Frontiera, A. I. Henry, J. A. Dieringer, and R. P. Van Duyne, Phys. Chem. Chem. Phys. **15**, 21 (2013).

[2] E. Petryayeva and U. J. Krull, Anal. Chim. Acta **706**, 8 (2011).

[3] S. Lal, N. K. Grady, J. Kundu, C. S. Levin, J. B. Lassiter, and N. J. Halas, Chem. Soc. Rev. **37**, 898 (2008).

[4] H. Wang, C. S. Levin, and N. J. Halas, J. Am. Chem. Soc **123**, 14992 (2005).

[5] J. P. Camden, J. A. Dieringer, J. Zhao, and R. P. Van Duyne, Acc. Chem. Res. **41**, 1653 (2008).

[6] L. B. Luo, L. M. Chen, M. L. Zhang, Z. B. He, W. F. Zhang, G. D. Yuan, W. J. Zhang, and S. T. Lee, J. Phys. Chem. C **113**, 9191 (2009).

[7] L. F. He, J. A. Huang, T. T. Xu, L. M. Chen, K. Zhang, S. T. Han, Y. He, and S. T. Lee, J. Mater. Chem **22**, 1370 (2012).

[8] S. Fayyaz, M. Tabatabaei, R. Hou, and F. Lagugne-Labarthet, J. Phys. Chem. C **116**, 11665 (2012).

[9] M. Ringler, T. A. Klar, A. Schwemer, A. S. Susha, J. Stehr, G. Raschke, S. Funk, M. Borowski, A. Nichtl, K. Kurzinger, R. T. Phillips, and J. Feldmann, Nano Lett. **7**, 2753 (2007).

[10] J. A. Huang, Y. Q. Zhao, X. J. Zhang, L. B. Luo, Y. K. Liu, J. A. Zapien, C. Surya, and S. T. Lee, Appl. Phys. Lett. **98**, 183108 (2011).

[11] Y. J. Oh and K. H. Jeong, Adv. Mater. **24**, 2234 (2012).

[12] E. C. Le Ru, E. Blackie, M. Meyer, and P. G. Etchegoin, J. Phys. Chem. C **111**, 13794-13803 (2007).

[13] K. Seo, M. Wober, P. Steinvurzel, E. Schonbrun, Y. Dan, T. Ellenbogen, and K. B. Crozier, Nano Lett. **11**, 1851 (2011).